# Ammonia combustion on a swirl and bluff body stabilized burner

Miguel Alexandre Coelho Franco
coelho.franco@tecnico.ulisboa.pt
Instituto Superior Técnico, Universidade de Lisboa, Portugal
January 2021

**Abstract**

Ammonia ($NH_3$) is a promising alternative to fossil fuels, however, its combustion presents challenges such as low flame speed, low temperature and high $NO_x$ emissions. Therefore, new systems are required to overcome these difficulties. In this work, a new burner for $NH_3$ combustion was designed, combining swirl and bluff-body recirculation, and tested for $NH_3/H_2$/air flames. Stability diagrams were obtained for 3 different thermal inputs to assess the operational range of the burner. Afterwards, $NO_x$ and $NH_3$ exhaust emissions were measured for 1.9 kW and for different equivalence ratios (φ) and $NH_3$ molar fractions in the fuel ($x_{NH_3}$), as well as measurements of temperatures, $NO_x$ and $O_2$ concentrations throughout the inside of the combustor. Good stability with relatively wide operational ranges were verified, increasing with the thermal input, including for pure ammonia/air flames, achieved only for 1.9 kW. Temperatures and $NO_x$ concentrations were higher in the recirculation zone. $NO_x$ concentrations increased with the increase of φ and with the decrease of $x_{NH_3}$. Also, $NO_x$ concentrations decreased along the combustor axis, where selective non-catalytic reduction (SNCR) is believed to occur. Globally, the burner presented good operational characteristics, producing a wide range of data. Moreover, this work opens perspectives on the use of this burner design in future ammonia gas turbines.

Keywords: Ammonia combustions, Swirl burner, Bluff-body flame stabilization, Experimental characterization, $NO_x$ concentrations, Laboratory-scale burner.

## 1. Introduction

There is an urgent need for new technologies to help the countries comply with the regulations imposed to reduce their greenhouse gas emissions. Renewable energy sources are a great way to oppose it, however their applicability is not as worldwide as desirable. Having that in mind, the need of fossil fuel alternatives for power generation has grown in the past years. It is in this scenario that ammonia ($NH_3$) appears as a good solution to substitute fossil fuels [1, 2]. Due to its carbon-free nature, ammonia will not produce $CO_2$ during combustion, having a lower impact in global warming than other conventional fuels. $NH_3$ production is well established, which combines nitrogen ($N_2$) with hydrogen ($H_2$), the latest coming mostly from natural gas reforming. However, new ways to get $H_2$ from renewable energy sources are being developed, reaching the so-called "green ammonia". Additionally, ammonia has been used for a long time, mainly as a fertilizer, meaning that a wide network for its production and transportation is already existed.

When compared to $H_2$, which is another promising alternative to fossil fuels, $NH_3$ has lower condensation pressure and is less reactive, which means that can be stored and transported in liquid form and at lower pressure, making it safer and easier to transport and store. Adding the fact that $NH_3$ production and distribution network is already widespread, these factors enhance its viability to be used and commercialized when compared to other options. Despite these advantages, $NH_3$ combustion has some drawbacks that soon became noticeable, such as its low flame speed, narrow flammability range, long ignition delay times and high $NO_x$ emissions [3–5]. $NH_3$ has also a problem inherent to its toxicity, limiting its use to technologies with good control of leak and unburned $NH_3$ emissions, and affecting the public and institutional acceptance of its viability.

After knowing the problems of burning ammonia, the scientific community started to develop and explore ways to overcome them. Naturally, the first

approaches were trying to use the same technologies used for other fuels. Some authors tried to use $NH_3$ in compression-ignition (CI) engines [6–8] and others in spark-ignition (SI) engines [9]. The findings were similar and conclude that pure $NH_3$ combustion was not possible. Some authors experimented ammonia blends with hydrogen [6, 9], methane [10], dimethyl ether [11, 12] and even diesel [7]. With these mixtures it was possible to burn high quantities of $NH_3$ improving the $CO_2$ emissions but increasing $NO_x$ emissions. Observing the better operability of $NH_3/H_2$ blends, which have enhanced flame speed and stability ranges than pure $NH_3$, some authors tried to create this mixture, only supplying $NH_3$ and cracking it before ignition [13].

The approaches that followed, were trying to create gas turbine burners with the purpose of burning ammonia. It was started by using swirl burners to improve mixing and stability, also improving the combustions characteristics [10, 14–17]. Hayakawa et al. [15] explored the effects of the equivalence ratio, finding that fuel-rich conditions generate high levels of $H_2$ while reducing $NO_x$ emissions. Following their work, Kurata et al. [16] claimed to be the first time that pure $NH_3$ power generation was achieved. They used a 50 kW micro gas turbine with a rich-lean staged of combustion approach and other combustions techniques. In their findings they conclude that this is the better way to achieve stable pure $NH_3$ combustion with low emissions.

In this context, this work presents and characterizes a new burner developed to burn ammonia. $NH_3/H_2$ fuel mixtures were used and the stability range of the burner was assessed first for 3 different thermal inputs and a range of molar fractions of $NH_3$ in the fuel. After that, using the higher thermal input, temperatures, $NO_x$ and $O_2$ concentrations were taken throughout the inside of the combustor for a range of equivalence ratios and $NH_3$ molar fractions in the fuel. $NO_x$ and $NH_3$ exhaust emissions were also analysed. All these measurements aimed to provide data for the $NH_3$ combustion literature and could be used for comparison and improvement of the numerical models used on this subject, as well as presenting a possible design for future gas turbines.

## 2. Material and methods

### 2.1 Combustor

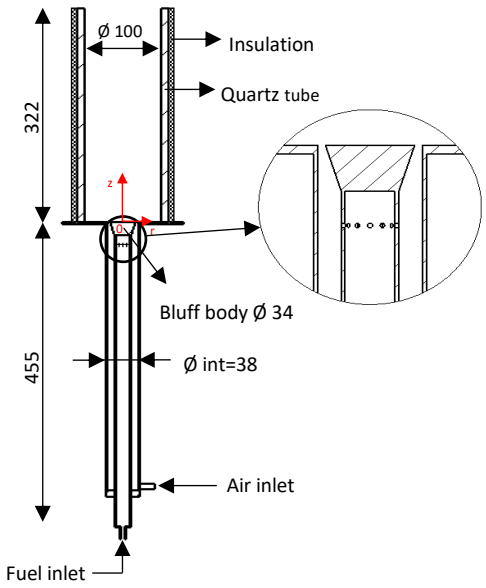


*Figure 1 – Schematic of the combustor with details of the bluff-body and injection zones. In red it is represented the axis used for the measurements. All values in mm.*

Figure 1 shows a schematic of the combustor, including details of the burner. The burner combines air swirl with a bluff-body to achieve better mixing and flame stability. It has two co-axial tubes for fuel and air injection. The swirl is created by the tangential air injection through 2 small tubes with internal diameter of 6 mm into the outer tube, with 38 mm of internal diameter, while the fuel (mixtures of $NH_2$ and $H_2$ ) runs through the inner tube, with outer diameter of 22 mm and thickness of 2 mm, being injected radially, through 12 holes with 2 mm of diameter, into the air stream 13.5 mm below the conical bluff body. The bluff body has a height of 20 mm, a base diameter of 22 mm and a top diameter of 34 mm. A quartz tube is placed on the top of the burner to confine the flame. This tube is insulated with ceramic wool to reduce heat losses. $NH_3$ and $H_2$ are fed to the burner from compressed bottles, while atmospheric air is injected from a compressor. Calibrated rotameters are used for controlling the air, $NH_3$ and $H_2$ flow rates.

### 2.2 Experimental techniques and uncertainties.

In the flame stability tests, the molar fraction of $NH_3$ in the fuel, $x_{NH_3}$, defined as $x_{NH_3} = V_{NH_3}/(V_{NH_3} + V_{H_2})$, was varied from 0.5 to 1 and 3 fixed thermal inputs (0.7, 1.3 and 1.9 kW) were investigated. To do so, volume flows of $NH_3$ and $H_2$ were kept constant for each condition, while the air flow was increased or decreased until extinction or unstable regime was detected visually, giving the maximum (rich limit) and the minimum (lean limit) equivalence ratio (ϕ) for each condition, respectively. Flashback was detected when the flame stabilized very near of the fuel injector holes. Each test was repeated, at least, 3 times, and repeatability was found adequate.

Gas sampling from inside the combustor was accomplished using a stainless steel, water-cooled probe with an inner diameter of ~1 mm. The probe was fixed on a structure that allowed for axial and radial movements within the combustor. The $O_2$ concentration measurements were performed using a magnetic pressure analyser (Horiba, model CMA-331A) and the $NO_x$ concentration measurements using a chemiluminescent analyser (Horiba, model CLA-510SS). The concentrations acquisition was made at 100 Hz for 30 seconds at least 6 times. For some conditions, dilution with $N_2$ was necessary to bring the $NO_x$ values within the analyser scale. At the exit of the combustor, in addition to the measurements of $O_2$ and $NO_x$ concentrations, Gastec detector tubes were employed to measure the emissions of $NH_3$. These tubes have a minimum detection limit of 2 ppm, while allowing for quantitative assessments starting at 10 ppm.

Temperatures inside the combustor were measured using a 76 µm diameter fine wire platinum/platinum-13% rhodium thermocouple mounted on a probe fixed on the same structure used for the gas species concentration measurements. The temperature data acquisition was made at 100 Hz for 30 seconds at least 3 times.

The maximum relative uncertainties for all the parameters evaluated in this work are represented in Table 1.

*Table 1 - Estimated uncertainties for the parameters evaluated.*

| Parameter evaluated | Uncertainty |
|---|---|
| $x_{NH_3}$ | 4.4 % |
| ϕ | 2% |
| temperature | 2% |
| $NO_x$ | 18% |
| $O_2$ | 14% |
| $NH_3$ | ± 50 ppm |

## 3. Results and discussion

### 3.1 Flame stability

In Figure 2 the results from the stability tests are represented. It is seen that for a given value of $x_{NH_3}$ the flame stays stable for a relatively wide range of values of ϕ, except for $x_{NH_3}$ > 0.9, a condition that was only achieved for the highest thermal input, 1.9 kW. When the thermal input increases, the stability range is improved, mainly due the increase of the rich limit. The widest range of equivalence ratios for all the thermal inputs was seen for $x_{NH_3}$ = 0.7. From that point, the rich limit decreases while increasing $x_{NH_3}$ due to the lower flame speed of the fuel mixture and decreases with the decrease of the $x_{NH_3}$ due the high content of $H_2$, which makes the mixture more reactive and causes flashback. In fact, for all the thermal inputs, for $x_{NH_3}$ < 0.7 flashback occurred while reaching the rich limit, while for the other conditions the flame has simply extinguished.

With increasing air, and thus decreasing equivalence ratio and increasing the velocity and the swirl intensity of the flow, the phenomenon of blow-out was observed below the minimum equivalence ratio for all conditions. Pure ammonia flames were achieved but the stability range narrows considerably, especially due to the higher lean stability limit, ϕ ≈ 0.8, but also due to the lower rich limit, ϕ ≈ 1.1. These results show the need for improvement of the burner to be able to burn pure ammonia flames, probably increasing the thermal input used would widen the stability range of those flames.

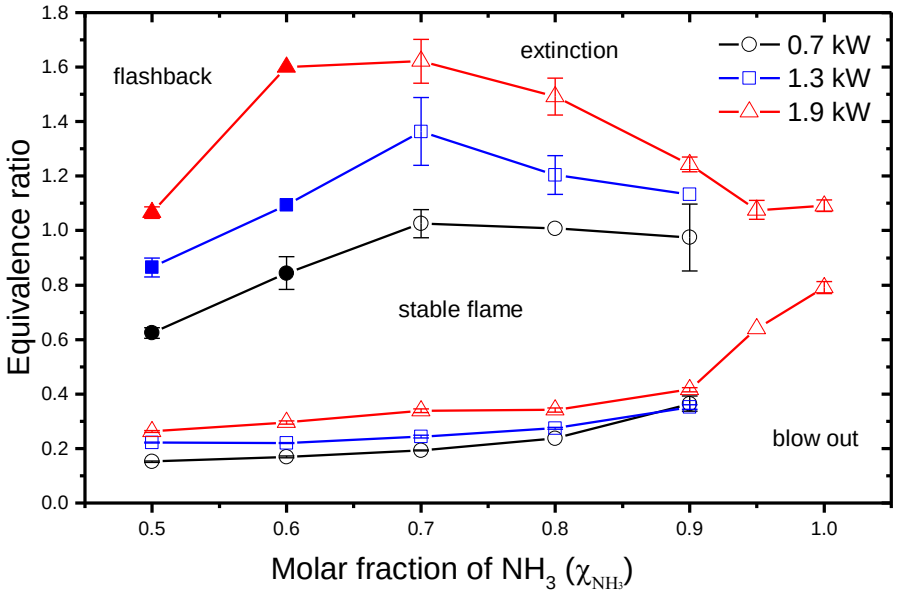


*Figure 2 - Stability diagram for the thermal inputs studied. Filled symbols refer to the points where flashback occurred.*

### 3.2 Test conditions and exhaust emissions

*Table 2 - Flame conditions and flue gas data. Thermal input for all flames was 1.9 kW.*

| Flame | $x_{NH_3}$ | $\phi$ | $NO_x$ (dry volume ppm @ 13% $O_2$) | $NH_3$ |
|---|---|---|---|---|
| 1 | 0.7 | 0.8 | 1302 | 14 |
| 2 | 0.8 | 0.8 | 806 | 16 |
| 3 | 0.9 | 0.7 | 248 | 75 |
| 4 | 0.9 | 0.8 | 628 | 13 |
| 5 | 0.9 | 0.9 | 661 | 15 |

After getting the stability across the thermal inputs, it was decided to work with the highest one, 1.9 kW and 5 flame conditions were defined to study and make the measurements. Altogether, they allow for an assessment of the effects of ϕ and $\chi_{NH_3}$ on the performance of the combustor. Table 2 shows the 5 flame conditions, also represented in Figure 3, and their exhaust values of $NH_3$ and $NO_x$.

Looking at the values, $NH_3$ emissions remain relatively low and close to each other, exception made for flame 3, which has a considerably higher value. $NO_x$ emissions decreased while increasing $\chi_{NH_3}$ and were similar while varying ϕ, exception made again for flame 3, which has lower value. Both results for flame 3 can be an indicator of poorer $NH_3$ conversion or incomplete combustion in this condition.

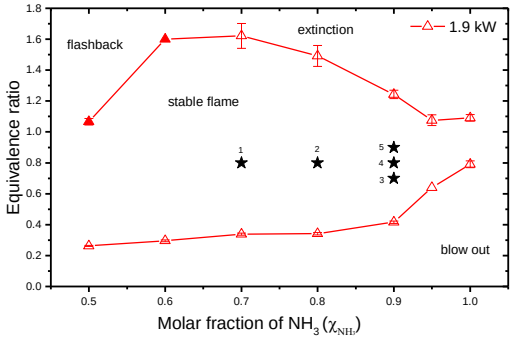


*Figure 3 - Stability diagram for 1.9kW. Stars represent the flame conditions studied for all the measurements listed in Table 2.*

As mentioned before, this work aimed to give an extensive data from the inside of the combustor, therefore all the measurements were taken for a "r" and "z" couple, being "r" the radial distance from the combustor center and "z" an axial distance from the bluff-body level. "r" values were varied from 0 to 30 mm with 5 mm of increment. The "z" values were varied with increasing increments downstream, being z= 30, 50, 70, 90, 120, 150, 200, 250 and 300 mm.

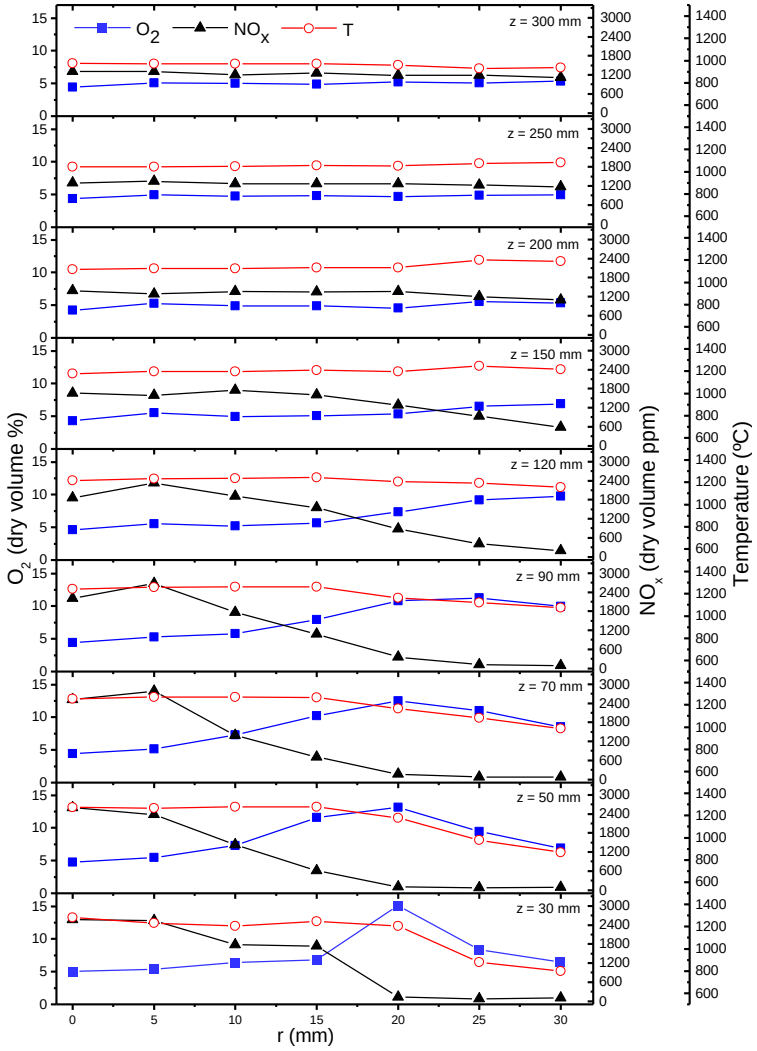


*Figure 4- Temperature, $NO_x$ and $O_2$ concentrations along the radius for all heights (z) studied. This graph represents the results for flame 4 ($x_{NH_3}$ =0.9 and φ = 0.8).*

### 3.3 In-flame data

In Figure 4 it is represented the temperature distribution, the $NO_x$ and $O_2$ concentrations across the radius (r) for all heights (z) for flame condition 4 ($x_{NH_3}$ = 0.9 and ϕ = 0.8), which are the conditions common both to ϕ and $x_{NH_3}$ variations studied.

Looking carefully to Figure 4, and focusing on the temperature profiles, it can be observed that temperatures, generally had a slight increase until z = 50 mm and decrease afterwards being in values possible for secondary reactions to occur. The maximum temperatures were recorded for z ≤ 50 mm and r ≤ 15 mm for all flame conditions, which can be considered inside the recirculation zone.

For r > 20 mm and z ≤ 90 mm lower temperatures were observed than for the other radial positions. From that height, the values for r > 20 mm started to be close to the other ones, being the temperature profile across the radius relatively constant for z's close to the exit of the combustor.

In Figure 5 the graphs are represented with the variation, for each z, of the temperature along the radius and a comparison between the equivalence ratios (a) and the molar fractions of $NH_3$ in the fuel (b) used. In the first graph (a) we can see that the temperature increases with the increase of the equivalence ratio. However, for most of the heights, the temperatures of ϕ=0.9 and ϕ=0.8 are closer when comparing to ϕ=0.7. This happens because while we are decreasing the equivalence ratio, we

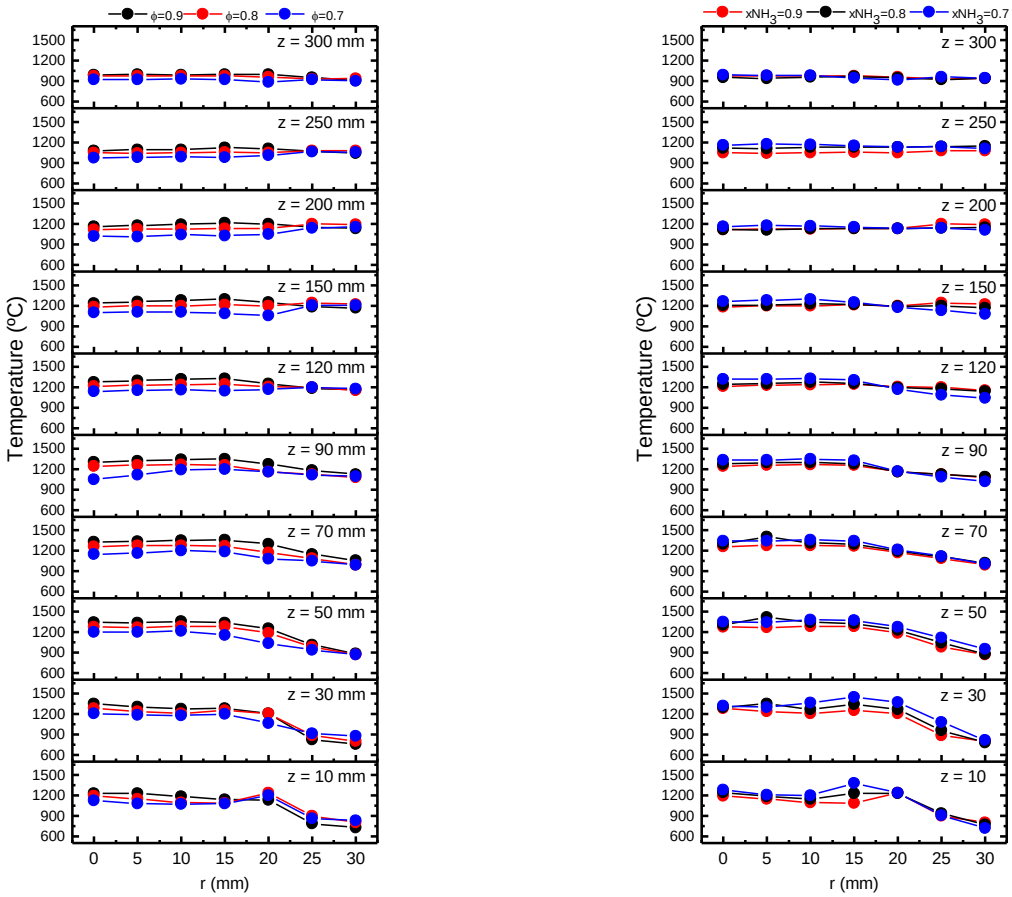


*Figure 5 – Temperatures along the r for each z. a) The curves represent the equivalence ratio variation at a fixed $NH_3$ molar fraction ($x_{NH_3} = 0.9$). b) The curves represent the variation of the $NH_3$ molar fraction in the fuel for a fixed equivalence ratio (ϕ=0.8).*

are subsequently increasing the air used for combustion, which means that there is more $O_2$ and $N_2$ during and after combustion, leading to reduced temperatures.

Observing the second graph (b), the temperatures are more similar between the flame conditions than the first one, only having more different values between the curves for z's closer to the bluff body. This is probably because we are using the same equivalence ratio, which gives a similar air flow rate and a similar afterburn concentrations of $O_2$ throughout the combustor. In general, the temperatures increase with the decrease of the $NH_3$ molar fraction in the fuel. This was expectable since in this way we are increasing the $H_2$ molar fraction, which is more reactive and has a higher flame temperature than $NH_3$, therefore increasing the flame temperature of the mixture.

Looking again to Figure 4, and focusing in $NO_x$ concentrations it is easily observable that, as for the temperatures, the $NO_x$ concentrations for r > 20 mm and z < 120 mm are much lower than for the other radial positions, since in this region there is no combustions and the temperatures are not enough to produce $NO_x$. Still regarding the $NO_x$, the higher values were recorded for what it was considered to be the recirculation zone, r < 20 mm and z < 120 mm, which is a zone with higher temperatures and higher concentration of combustion products, in this case $NO_x$. The concentration of $NO_x$ increased while getting closer to the bluff body and the center of the combustor. After z = 120 mm the $NO_x$ differences between the center and the other radial positions starts to decrease being almost constant at the exit.

For r < 20 mm, a decrease of $NO_x$ concentration can be seen across the axial axis (z), which could be explained by species diffusion caused by the flow, however, it may not be the only mechanism occurring there. For z > 70 mm, in theory, selective non-

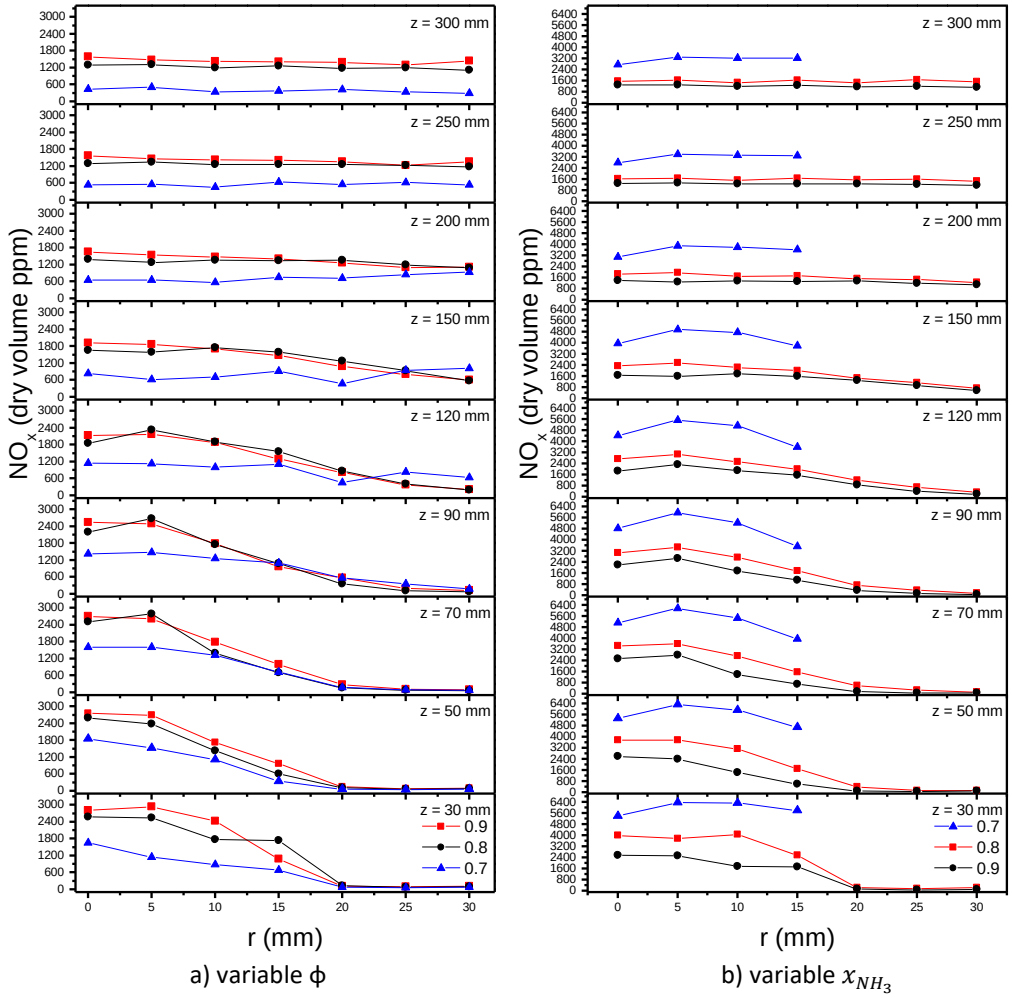


*Figure 6 – $NO_x$ profiles along the radius (r) for all heights (z). (a) conditions with the same $NH_3$ molar fraction ($x_{NH_3}$ =0.9) and (b) conditions with the same equivalence ratio (ϕ = 0.8).*

catalytic reduction (SNCR) could be taking place, where some ammonia that had not been consumed in combustion may be consumed in this region reducing $NO_x$, since the temperatures are in favourable values for this phenomenon to happen.

In an attempt to assess the symmetry of the flames, temperature measurements were made for symmetrical radial position, relative to the combustor axis. It was found that the values had small differences between each other, only few points having more significant discrepancies. These findings help to conclude that, due to the nature of the flow of this burner, there is reasonably good symmetry on the flame.

Still analysing Figure 4 and looking to the $O_2$ profiles, it can be seen that, like $NO_x$ concentrations, for z > 120 mm the $O_2$ concentration tends to stabilize across the radial positions becoming relatively constant. For z < 120 mm we can notice 3 different behaviors. For r < 20 mm the values of $O_2$ remain low, slightly increasing across the radius. As mentioned, this region corresponds to the recirculation zone, therefore it was expected that the $O_2$ concentration was low. For r = 20 mm, there is a peak of the $O_2$. This radius is near the injection zone of the reactants which mean that, depending on the condition and the height, the maximum $O_2$ is recorded for this radius because the combustion is not happening yet in this region making the $O_2$ injected in there not yet consumed. This peak was observed at r = 20 mm for all flames. For r > 20 mm, $O_2$ concentration decreases again, being slightly higher than the values for r < 20 mm. This could happen due to the fact that this is a zone outside the recirculation zone, where there is no combustion and there is

some non-consumed $O_2$ from the reactants present there.

In Figure 6 it is represented a comparison of the $NO_x$ concentrations while varying the ϕ (Figure 6 (a)) and the $x_{NH_3}$ (Figure 6 (b)). Looking to Figure 6 (a) it can be seen that the profile tendencies for ϕ = 0.8 and ϕ = 0.9 are similar being the values pretty close between them, and overall higher for ϕ = 0.9, verifying only a greater difference for the zone of r < 20 mm and z < 70 mm. For ϕ = 0.7, the tendency for lower z's is much different from the other 2 conditions and the values for all heights are considerably lower. This fact could indicate that, for some reason, incomplete combustion could be happening which would mitigate $NO_x$ production during the combustion process. On the other hand, an incomplete combustion, in theory, would lead to a higher amount of unburned fuel in the products which could be the same to say higher amount of $NH_3$. This theoretical increase of $NH_3$ presence in the products could improve the SNCR intensity reducing the already lower concentration of $NO_x$.

Looking now to Figure 6 (b), it is worth mentioning that for flame 1 (blue line), measurements were not completed due to technical issues with the analyser, but for comparison, the measured values are presented here. Comparing the flames 2 (red line) and 4 (black line), it can be seen that the tendencies are very similar to each other on every height (z), being the values for flame 2 always higher than flame 4. However, for the recirculation zone (r < 20 and z < 70), the difference between the values is considerably higher than in the other regions. Also, it can be seen that, for flame 1, the values of $NO_x$ concentration are much higher for all measured points than for the other flames, being the difference between flame 1 and 2 also much higher than between flame 2 and 4. This increase on $NO_x$ concentration with the decrease of $NH_3$ molar fraction in the fuel ($x_{NH_3}$) observed here is directly correlated with the fact that while decreasing the quantity of $NH_3$, in this dual fuel approach adopted for this work, it is increased the quantity of $H_2$ present in combustion. The increase of $H_2$ concentration in the fuel makes the mixture more reactive due to the $H_2$ higher reactivity, higher flame speed and higher flame temperature than $NH_3$. This increase in the mixture reactivity will increase the generation of OH and O radicals due to the $H_2$ oxidation pathways. These radicals are fundamental for the HNO pathway, which is the most important on the NO formation [18, 19]. In this way the increase of $H_2$ in the fuel mixture will lead to higher intensity in the chemistry behind $NO_x$ formation increasing the values of $NO_x$ concentration.

The same kind of comparisons made in Figure 6 can be made for $O_2$ concentrations. Generally, the profiles have similar tendencies for all the flames. As expected, the $O_2$ concentrations increased while decreasing the ϕ because of the higher excess air used for combustion. While varying the $x_{NH_3}$, the $O_2$ concentration profiles remain very close to each other, mainly due the fact that they all have the same equivalence ratio, therefore the amount of air used for combustion are very similar resulting in similar afterburn $O_2$ concentrations. For all flames, the profiles near the exit are practically constant.

Overall, the developed burner worked well for the proposed study showing good stable operation conditions. The flame was stable during all the extensive measurements done in the scope of this work. The burner revealed to work well with high amounts of $NH_3$ in the fuel mixture and with good emissions for some of the conditions.

## 4. Closure

### 4.1 Conclusions

The main conclusions from this work can be summarized as follows:

- Stability tests showed relatively wide operational ranges for all $x_{NH_3}$ and for all thermal inputs. The stability increased with the thermal input and the maximum ϕ was verified for $x_{NH_3}$ = 0.7 in all of them.
- Pure ammonia flame was achieved only for 1.9 kW, but still with narrow operational range.
- Maximum temperatures were recorded for z ≤ 50 mm and r ≤ 15 mm, which is inside the recirculation zone. Temperature decreases with the decrease of the equivalence ratio, due to the higher concentration of $O_2$ and $N_2$ during combustion and increases with the decrease of $x_{NH_3}$ due to the higher reactivity and flame temperature of $H_2$

- Exhaust measurements showed that $NO_x$ emissions increase with the decrease of the $x_{NH_3}$. While varying the equivalence ratio, exhaust $NO_x$ was relatively similar exception made for flame 3 ($x_{NH_3}$ = 0.9 and ϕ = 0.7), which gave a lower value. Exhaust ammonia was found low, except for flame 3, which gave a relatively high value.
- $O_2$ concentrations inside the combustor were similar while varying $x_{NH_3}$ and increased with the decrease of ϕ, having all the flames a peak of $O_2$ at r = 20 mm. $NO_x$ concentrations were higher inside the recirculation zone and for lower z's. There was a decrease of $NO_x$ concentrations along the axis (z) due to the species diffusion and SNCR mechanism, since the temperatures along the combustor are in possible values for that to happen.
- $NO_x$ concentrations decrease with the decrease of the equivalence ratio however, they are close for ϕ = 0.9 and 0.8 and considerably lower for ϕ = 0.7. Also, they increase with the decrease of $x_{NH_3}$ due to the higher content of hydrogen, which prompts the generation of OH and O radicals that favours the NO formation.

### 4.1 Recommendations for future work

Despite the success of the burner operation, some improvements, modifications and different techniques can be applied.

Using different techniques to measure species and temperatures would be of great interest because the ones used in this work are intrusive techniques which certainly will interfere with the flame. In this way it will be possible to assess the influence of the probes in the values obtained. Moreover, with different techniques it could be possible to measure different species rather than $NO_x$ and $O_2$ inside the flame which are of interest for better understanding of what is happening in the combustion zone.

Also, to optimize operational conditions, the burner should be tested with higher thermal inputs, either to see the maximum supported and to see if it can be obtained wider stability for pure ammonia.

To reduce $NO_x$ emissions and production, this burner could be tested in rich regime, differently from the lean regime that was used in this work, which is known to have lower $NO_x$ emission. However, emission of unburned ammonia must be careful assessed, which could be dangerous and threatening for humans. Despite this, using a rich regime in this combustor, in theory could open the possibility of using a second stage of combustion after the exit of the combustor. This would make it possible to, for example, inject a second combustion air and burn the unburnt fuel from the first stage. If necessary, air and fuel could be injected in the second stage to help to stabilize the secondary flame. In this way $NO_x$ production could be reduced in the first stage and produce lower concentrations of $NO_x$ in the lean secondary stage while having near zero unburned fuels.

Regardless of all these possibilities, this burner is a laboratory scale combustion rig so that the applicability of the techniques employed here should be investigated when applied to practical industrial size burners that can be used, for example, in gas turbines for electricity production.

## References


[1] H. Kobayashi, A. Hayakawa, K. D. K. A. Somarathne, and E. C. Okafor, "Science and technology of ammonia combustion," *Proc. Combust. Inst.*, vol. 37, no. 1, pp. 109–133, 2019, doi: 10.1016/j.proci.2018.09.029.

[2] A. Valera-Medina, H. Xiao, M. Owen-Jones, W. I. F. David, and P. J. Bowen, "Ammonia for power," *Prog. Energy Combust. Sci.*, vol. 69, pp. 63–102, 2018, doi: 10.1016/j.pecs.2018.07.001.

[3] E. Kroch, "Ammonia - A fuel for motor buses," *Jounal Inst. Pet.*, vol. 31, pp. 213–223, 1945.

[4] E. S. Starkman and G. S. Samuelsen, "F L A M E - P R O P A G A T I O N RATES IN A M M O N I A - A I R C O M B U S T I O N AT H I G H P R E S S U R E," *Symp. Combust.*, vol. 11, no. 1, pp. 1037–1045, 1967.

[5] D. T. Pratt, "Performance of ammonia-fired gas-turbine combustors," *Army Mater. Command 2 D Dir. Chem. Mater. Branch*, 1967.

[6] S. S. Gill, G. S. Chatha, A. Tsolakis, S. E. Golunski, and A. P. E. York, "Assessing the effects of partially decarbonising a diesel engine by co-fuelling with dissociated ammonia," *Int. J. Hydrogen Energy*, vol. 37, no. 7, pp. 6074–6083, 2012, doi: 10.1016/j.ijhydene.2011.12.137.

[7] A. J. Reiter and S. C. Kong, "Demonstration

of compression-ignition engine combustion using ammonia in reducing greenhouse gas emissions," *Energy and Fuels*, vol. 22, no. 5, pp. 2963–2971, 2008, doi: 10.1021/ef800140f.

[8] A. J. Reiter and S. C. Kong, "Combustion and emissions characteristics of compression-ignition engine using dual ammonia-diesel fuel," *Fuel*, vol. 90, no. 1, pp. 87–97, 2011, doi: 10.1016/j.fuel.2010.07.055.

[9] J. H. Lee, S. I. Lee, and O. C. Kwon, "Effects of ammonia substitution on hydrogen/air flame propagation and emissions," *Int. J. Hydrogen Energy*, vol. 35, no. 20, pp. 11332–11341, 2010, doi: 10.1016/j.ijhydene.2010.07.104.

[10] A. Valera-Medina *et al.*, "Ammonia, Methane and Hydrogen for Gas Turbines," *Energy Procedia*, vol. 75, pp. 118–123, 2015, doi: 10.1016/j.egypro.2015.07.205.

[11] K. Ryu, G. E. Zacharakis-Jutz, and S. C. Kong, "Performance characteristics of compression-ignition engine using high concentration of ammonia mixed with dimethyl ether," *Appl. Energy*, vol. 113, pp. 488–499, 2014, doi: 10.1016/j.apenergy.2013.07.065.

[12] C. W. Gross and S. C. Kong, "Performance characteristics of a compression-ignition engine using direct-injection ammonia-DME mixtures," *Fuel*, vol. 103, pp. 1069–1079, 2013, doi: 10.1016/j.fuel.2012.08.026.

[13] K. Ryu, G. E. Zacharakis-Jutz, and S. C. Kong, "Performance enhancement of ammonia-fueled engine by using dissociation catalyst for hydrogen generation," *Int. J. Hydrogen Energy*, vol. 39, no. 5, pp. 2390–2398, 2014, doi: 10.1016/j.ijhydene.2013.11.098.

[14] A. Valera-Medina, D. G. Pugh, P. Marsh, G. Bulat, and P. Bowen, "Preliminary study on lean premixed combustion of ammonia-hydrogen for swirling gas turbine combustors," *Int. J. Hydrogen Energy*, vol. 42, no. 38, pp. 24495–24503, 2017, doi: 10.1016/j.ijhydene.2017.08.028.

[15] A. Hayakawa, Y. Arakawa, R. Mimoto, K. D. K. A. Somarathne, T. Kudo, and H. Kobayashi, "Experimental investigation of stabilization and emission characteristics of ammonia/air premixed flames in a swirl combustor," *Int. J. Hydrogen Energy*, vol. 42, no. 19, pp. 14010–14018, 2017, doi: 10.1016/j.ijhydene.2017.01.046.

[16] O. Kurata *et al.*, "Development of a wide range-operable, rich-lean low-NOx combustor for NH 3 fuel gas-turbine power generation," *Proc. Combust. Inst.*, vol. 37, no. 4, pp. 4587–4595, 2019, doi: 10.1016/j.proci.2018.09.012.

[17] E. C. Okafor *et al.*, "Towards the development of an efficient low-NOx ammonia combustor for a micro gas turbine," *Proc. Combust. Inst.*, vol. 37, no. 4, pp. 4597–4606, 2019, doi: 10.1016/j.proci.2018.07.083.

[18] R. C. Rocha, C. F. Ramos, M. Costa, and X. S. Bai, "Combustion of NH3/CH4/Air and NH3/H2/Air Mixtures in a Porous Burner: Experiments and Kinetic Modeling," *Energy and Fuels*, vol. 33, no. 12, pp. 12767–12780, 2019, doi: 10.1021/acs.energyfuels.9b02948.

[19] R. C. da Rocha, M. Costa, and X. S. Bai, "Chemical kinetic modelling of ammonia/hydrogen/air ignition, premixed flame propagation and NO emission," *Fuel*, vol. 246, no. December 2018, pp. 24–33, 2019, doi: 10.1016/j.fuel.2019.02.102.